



# International Journal of Pharmacology

ISSN 1811-7775

**science**  
alert

**ansinet**  
Asian Network for Scientific Information



## Research Article

# Atorvastatin-TPGS-PLGA Nanoparticles Cytotoxicity Augmentation Against Liver Cancer HepG2 cells

<sup>1</sup>Mohammad Y. Alfaifi, <sup>1</sup>Ali A. Shati, <sup>1</sup>Mohammed Ali Alshehri, <sup>1,2</sup>Serag Eldin I. Elbehairi, <sup>3</sup>Usama A. Fahmy and <sup>4</sup>Ohoud Yahya Alshehri

<sup>1</sup>Department of Biology, Faculty of Science, King Khalid University, 9004 Abha, Saudi Arabia

<sup>2</sup>Laboratory of Cell Culture, Egyptian Organization for Biological Products and Vaccines (VACSERA Holding Company), 51 Wezaret El-Zeraa Street, Agouza, Giza, Egypt

<sup>3</sup>Department of Pharmaceutics, Faculty of Pharmacy, King Abdulaziz University, P.O. Box 80260, Zip Code 21589, Jeddah, Saudi Arabia

<sup>4</sup>Department of Biochemistry, Faculty of Science, King Abdulaziz University, Jeddah, Saudi Arabia

## Abstract

**Background and Objective:** Reports revealed atorvastatin (ATR) exerts significant anti proliferative properties against cancer cell lines. Aim of this study was the potentiation of ATR cytotoxic effects against HepG2 cells by using TPGS as a surfactant and loading on PLGA NPs. **Materials and Methods:** Nanoprecipitation method was used to trap ATR within PLGA nanoparticles, the method uses vitamin E TPGS as an emulsifier. The nanoparticles' encapsulation efficiency, size, zeta potential (ZP), surface morphology and *in vitro* drug release were evaluated. **Results:** The mean size of the particles was  $176.2 \pm 14.1$  nm, they had a ZP of  $-15.1 \pm 4.4$  mV and polydispersity index of 0.32 and after 12 h, approximately 96% of raw ATR had dissolved in comparing with 25% of raw ATR. It was found that ATR-NPs was twice as cytotoxic as the raw ATR. In both instances, for HepG2 cells cycle analysis accumulated at the pre-G1 apoptotic phase in response to ATR and ATR-NPs. Indeed, increase of cells at pre-G1 initiated by ATR 4.45 times the normal level, rising to a 24.05-fold increase for ATR-NPs. The ATR annexin V-FITC apoptosis assay showed significant increase in the amount of annexin V-FITC positive apoptotic cells (both early and late apoptosis) in HepG2 cells treated with ATR-NPs. **Conclusion:** These findings suggested that this formula is a promising therapy for patients with liver cancer.

**Key words:** Statins, cellular uptake, nanoparticles, drug delivery, liver cancer, cytotoxicity

**Citation:** Mohammad Y. Alfaifi, Ali A. Shati, Mohammed Ali Alshehri, Serag Eldin I. Elbehairi, Usama A. Fahmy and Ohoud Yahya Alshehri, 2020. Atorvastatin-TPGS-PLGA nanoparticles cytotoxicity augmentation against liver cancer HepG2 cells. *Int. J. Pharmacol.*, 16: 79-86.

**Corresponding Author:** Usama A. Fahmy, Department of Pharmaceutics, Faculty of Pharmacy, King Abdulaziz University, P.O. Box 80260, Zip Code 21589, Jeddah, Saudi Arabia

**Copyright:** © 2020 Mohammad Y. Alfaifi *et al.* This is an open access article distributed under the terms of the creative commons attribution License, which permits unrestricted use, distribution and reproduction in any medium, provided the original author and source are credited.

**Competing Interest:** The authors have declared that no competing interest exists.

**Data Availability:** All relevant data are within the paper and its supporting information files.

## INTRODUCTION

The World Health Organization cites cancer is one of the world's leading causes of mortality, accounting for approximately 13% of all deaths<sup>1,2</sup>. There are a number of problems commonly associated with cytotoxic agents, including having poor specificity and stability, being toxic to normal, healthy cells, whilst tumor cells are often resistant to the drugs<sup>3,4</sup>. The cytotoxic agents that are given through traditional routes act widely, unpredictably and without specificity, binding to healthy serum proteins and body tissues<sup>5-7</sup>. Only a small amount of the drug administered reaches the tumor, limiting the efficacy of the drug and simultaneously causing widespread toxicity<sup>5,8</sup>. Cytotoxic drugs act indiscriminately, although intended to kill cancer cells only, they do not distinguish between cancerous and non-cancerous cells, in particular affecting cells that undergo rapid division, such as bone marrow cells and gastrointestinal tract cells<sup>9</sup>. The damage to normal tissue is not dose-dependent, as even standard doses of anticancer drugs cause toxicity. Effective cancer treatments are persistently challenged by the bio-distribution, pharmacology and poor specificity of cytotoxic anticancer drugs, which has significant implications for the drugs' therapeutic values. Statins inhibit HMG-CoA reductase, this protein is the enzyme that limits the rate of mevalonate synthesis<sup>10,11</sup>. This metabolic pathway synthesizes cholesterol precursors. As well as inhibiting cholesterol biosynthesis, it seems that statins exert pleiotropic effects modulating diverse cellular processes, such as apoptosis, cell growth and inflammation. Statins can exert considerable influence upon the progression of diseases, such as cancer, as they adjust these processes and pathways<sup>12</sup>. *In vitro* studies of various cell lines indicates that statins exhibit cancer inhibiting effects on different cell lines by inhibiting apoptosis, cell proliferation and mevalonate biosynthesis<sup>13</sup>. The synthetic statin, ATR was designed for and is commonly used to treat hypercholesterolemia. Following oral administration, the maximum plasma concentrations of ATR is achieved within 1-2 h, demonstrating its rapid absorption<sup>14-16</sup>. The absolute bioavailability of ATR is low, around 14%, resulting from gastrointestinal mucosa clearance and hepatic first-pass metabolism. Yet the inhibitory activity from the systemic availability of HMG-CoA reductase<sup>17</sup> is approximately 30%. Polymeric nanoparticles (PNPs) are colloidal particles of submicron sizes. They can be used to deliver anticancer agents that are adsorbed or contained within or conjugated to the PNP surface. By loading PNPs with appropriate anticancer therapeutic agents, PNPs can be targeted to deliver their cargos to specific sites then release

their contents over a prolonged duration. Targeted drug delivery system (TDDS) is a new development that exploits the rational design features of polymers, including stability, composition, crystallinity, hydrophobicity, molecular weight, polydispersity and solubility<sup>18</sup>. The polymers used in TDDS are custom-made to accommodate the charge and molecular weight of a particular cargo). The FDA-approved copolymer of lactic acid and glycolic acid, poly-(lactic-co-glycolic acid) (PLGA) is a biocompatible, biodegradable, nontoxic and synthetic polymer. Although there are a number of published studies describing PLGA-loaded NPs, these are largely restricted to *in vitro* evaluations and there is limited research addressing the use of PLGA-based NPs to target active tumors either *in vitro* or *in vivo*<sup>19-22</sup>. The amphiphilic compound, vitamin E TPGS, which is a form of vitamin E, has a hydrophilic PEG chain and a hydrophobic vitamin E component making it miscible in water. Its structure facilitates excellent drug delivery. The evidence from in-depth research suggests that TPGS has considerable potential to inhibit P-gp, exerting selective, anti-tumor effects<sup>23-25</sup>. The aim of this work was the potentiation of ATR cytotoxic effects against HepG2 cells by using TPGS as a surfactant. This study represented a novel work which includes using combined ATR and TPGS as a drug and surfactant, both of them have cytotoxic effect loaded on a biodegradable polymer, then evaluating the cytotoxic properties of this combination, these findings will open the way for new uses and recommendation for statins uses.

## MATERIALS AND METHODS

**Materials:** Atorvastatin calcium (raw-ATR) was gifted by DEEF pharmaceuticals (Al-Qaseem, Saudi Arabia). Poly-(lactic-co-glycolic acid) (PLGA, Mw 7,000-17,000) and D- $\alpha$ -Tocopherol polyethylene glycol 1000 succinate (TPGS) were purchased from Sigma-Aldrich (St. Louis, Missouri, United States of America). This study was carried out at the faculty of Pharmacy, King Abdul-Aziz university, Jeddah, Saudi Arabia in the period from January to September, 2019.

### Methods

**Formulation of ATR-NPs:** To prepare ATR-NPs, single emulsion and evaporation method<sup>26</sup> was used. A solution of dichloromethane solvent and ATR, PLGA in ratio (1:1), dissolved in 5 mL of the solution. A probe sonicator (Ultrasonic Processor, gx-130, Berlin, Germany) was used to emulsify the organic phase to an aqueous phase (TPGS, 0.5% w/v), sonication was applied for 3 min at 25°C with 60% voltage efficiency. To remove the dichloromethane, the

organic solvent was evaporated in a vacuum at 40°C. Then centrifugation at 50,000 rpm was used for 20 min to separate the ATR-NPs from the bulk aqueous phase. The NPs were then washed 3 times in distilled water and freeze-dried.

**Particle size (ZP) and poly dispersity index (PDI):** After freeze-drying the NPs, they were dispersed in Milli-Q water. Using the dynamic light-scattering technique, the particle size, polydispersity index (PDI) and ZP of the suspension were ascertained. To measure the mean particle size and the PDI of the aqueous dispersion the Malvern Particle Size Analyzer (Malvern Instruments Ltd, Holtsville, NY, USA) was used. To do that, 3 mL of each sample was transferred in transparent disposable plastic cassettes. To obtain the ZP measurements of ATR- NPs, the same analyzer was used as glass electrode. Using deionized water, NP samples were diluted to 200 times and sonicated for 10 min<sup>27</sup>.

**Determination of drug entrapment efficiency (EE (%)):** To establish the drug entrapment efficiency (EE (%)) of ATR in the PLGA NPs, the indirect method was adopted. A transparent supernatant was obtained by centrifuging the freshly prepared emulsion was centrifuged at 12,000 rpm for 10 min. The content of drug in the supernatant that was not encapsulated was measured by UV spectroscopy at 245 nm<sup>28</sup>. The percentage of EE was calculated as follows<sup>29</sup>:

$$EE (\%) = \frac{\text{Drug added} - \text{Free drug}}{\text{Drug added}} \times 100$$

**Particle morphology by SEM:** A scanning electron microscope was used to examine the morphology of the optimized ATR- NPs. Under vacuum conditions, a sputter coater applied a 2-20 nm layer of metals such as gold, palladium or platinum to the freeze-dried PLGA NPs. Then the coated specimens were bombarded with an electron beam to produce auger electrons. Electrons scattered, which scattered at an angle equal to or exceeding 90° were selected and processed further<sup>29</sup>.

**Drug-release studies:** To determine the pattern of drug release from ATR- NPs, an *in vitro* drug-release study was conducted. Briefly, pure ATR and lyophilized NPs were dispersed in a dialysis tube (molecular weight cut-off 12 kDa) containing phosphate buffer (pH 6.8). The tube was put into a biological shaker (LBS-030S-Lab Tech, Korea) and shaken horizontally at 100 rpm at 37°C. The supernatant was drawn off<sup>30</sup> at 1, 2, 3, 4, 6, 8 and 12 h. The remaining sample was centrifuged for 5 min at 12,000 rpm. The UV spectroscopy was used at 239 nm to analyze the drug content.

**MTT assay:** A 3-(4,5-Dimethylthiazol-2-yl)-2,5-diphenyltetrazolium bromide (MTT) assay was performed to evaluate the viability of HepG2 cells exposed to NPs of each size at concentrations of 10-500 µg mL<sup>-1</sup> for 24 and 72 h. Further details are supplied in the supplementary materials. The lactate dehydrogenase (LDH) leakage was determined from cells exposed to 20-200 nm SNPs at concentrations of 10-500 µg mL<sup>-1</sup> for 24 or 72 h (Supplementary Materials). Using fluorogenic probes Intracellular ROS and cellular glutathione (GSH) levels were determined from cells exposed to 20, 60, 100 and 200 nm SNPs at concentrations of 50, 100, 200 and 500 µg mL<sup>-1</sup> for 24 h<sup>31</sup>.

**Cell cycle progression analysis:** Flow cytometer was used to determine the distribution of DNA in the cell cycle. Six-well cell culture plates were seeded with approximately 3×10<sup>5</sup> cells/well. Cells were exposed to different concentrations of ATR- NPs (10-80 µg mL<sup>-1</sup>) for 6, 24 and 48 h. Treatment was removed, the cells were collected then they were centrifuged at 135 g at 37°C for 10 min. The pellet was fixed in ice-cold ethanol (70% in 1× PBS) and incubated for 30 min at -20°C. Cells were then centrifuged again and re-suspended in lysis buffer (0.2% triton in 1× PBS) and incubated for 30 min at 4°C. Cells were further centrifuged and re suspended in 20 µg mL<sup>-1</sup> RNase prepared in 1× PBS, then incubated for 30 min at 37°C. Cells were centrifuged one more time before re-suspending them in 1× PBS and then staining them with 10 µL PI (1 mg mL<sup>-1</sup>). The cells were incubated at 4°C until required for flow cytometry analysis (FACSCalibur, BD Bioscience)<sup>31</sup>.

**Caspase-3 enzyme assay:** Formula free of the drugs, ATR and ATR-NPs were tested. To evaluate caspase-3 activity, cells were grown at 37°C in RPMI 1640 containing 10% FBS. They were then lysed with a cell extraction buffer. Using standard diluent buffer, the lysate was diluted over the range of the assay. To measure the content of the active caspase-3, 100 µL of each cell sample and 100 µL complete growth medium were combined then plated on 96-well plates at a density of 1.2-1.8×10,000 cells/well. These were incubated for 24 h. Spectrophotometry of the samples was performed at 450 nm according to manufacturer's (USCN Life Science Inc., China)<sup>31</sup>.

**Statistical analysis:** The statistical analysis were performed with the IBM SPSS statistics software, version 25 (SPSS Inc., Chicago, IL, USA). The comparison of means was performed using an Analysis of variance (ANOVA) followed by Tukey as a *post hoc* test. The data are presented as the Mean±SD. The differences were considered significant at p<0.05.

## RESULTS

The SEM image in Fig. 1 illustrates homogeneously sized, spherical NPs with smooth edges. Table 1 represents the average particle size of prepared ATR-NPs was  $176.2 \pm 14.1$  nm, the ZP was  $-15.1 \pm 4.4$  mV and the polydispersity index was 0.32. The ATR (%) EE of the prepared NLCs was  $91.2 \pm 2.3\%$ , Fig. 2 shows the percentage of ATR that diffused from the prepared ATR-NPs formula compared with the raw ATR. At 12 h, the diffusion of the raw ATR was 35% of the total raw ATR dissolved in the medium at the end of this experiment. However, the ATR-NPs demonstrated an improved ATR permeation pattern, which reached a value of  $96.80 \pm 3.12\%$ . Figure 2 presents the release of ATR. After 1 h, the dissolution rate of the ATR suspension was approximately 80%, which is normal because there are no solid carries. In contrast, there was an initial spurt of release for the ATR-NPs but this changed to become a slow release. The ATR trapped deep within the ATR-NPs was influenced by the composition and qualities of the lipid carrier, the particle size and the pH of the medium. Fig. 3 shows cell viability was reduced in a dose-dependent manner in all treatments. All treatments reduced cell viability in a dose-dependent manner. The  $IC_{50}$  values for the treatments were as follows: ATR,  $23.2 \pm 3.2 \mu\text{M}$ , ATR-NPs  $4.44 \pm 0.21 \mu\text{M}$ . While TPGS  $11.2 \pm 2.2 \mu\text{M}$  as shown in Fig. 3.

**In vitro DNA flow cytometric analysis:** As shown in Table 2, cell cycle analysis results indicated that, the HepG2 cells accumulated in the G2/M phase which was an indicate to cellular DNA damage. The HepG2 cells treated with ATR-NPs accumulated by 45.04% in comparing with 26.43% cells treated with raw ATR in the G2/M phase. While in the pre G1 phase, which revealed to cell death, 26.08% of the cells died after treatment with ATR-NP<sub>3</sub> in comparing with 7.26% of cells treated with raw ATR. To further, substantiate the observed cell apoptotic death, the percentage of cells with positive annexin-V staining was assessed in the control, ATR, TPGS and ATR- NPs incubations (Fig. 4a-d). The ATR- NPs obviously increased the early, late and total cell death when compared to all the other incubations. Figure 4 is a graphical illustration for each type of cell death. The observed apoptotic cell death induced by the ATR-NPs was further confirmed by determining the caspase 3 content.

**Caspase-3 enzyme assay:** The cells exposed to the ATR-NPs showed the highest content of caspase 3 ( $671.2 \pm 111 \text{ pg mL}^{-1}$ ) when compared to the control ( $79.66 \pm 25.1 \text{ pg mL}^{-1}$ ), raw ATR ( $324.3 \pm 96.5 \text{ pg mL}^{-1}$ ) and TPGS ( $418 \pm 119.52 \text{ pg mL}^{-1}$ ) incubations (Fig. 5).

Table 1: ATR-NP characterization parameters

Parameter	Size (nm)	ZP (mV)	PDI	EE (%)
ATR-NPs	$176.2 \pm 14.1$	$-15.1 \pm 4.4$ mV	$0.32 \pm 0.01$	$91.2 \pm 2.3$

mV: Milli volt, PDI: Poly dispersity Index, ZP: It's a measure of the electrical charge of particles, EE (%): Drug entrapment efficiency

Table 2: Cell cycle phases after ATR, ATR-NPs and TPGS treatments

Cell phase	G0-G1 (%)	S (%)	G2-M (%)	Pre G1 (%)
Control	54.26	33.15	12.59	1.63
ATR-NPs	31.24	23.72	45.04	26.08
ATR	43.95	29.62	26.43	7.26
TPGS	48.93	27.52	23.55	15.29

G0-G1, S, G2-M, Pre-G1: Phases of cell cycle

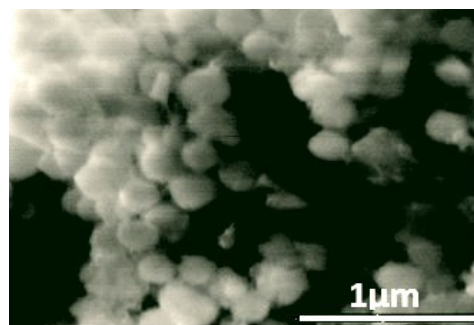


Fig. 1: ATR-NPs SEM image

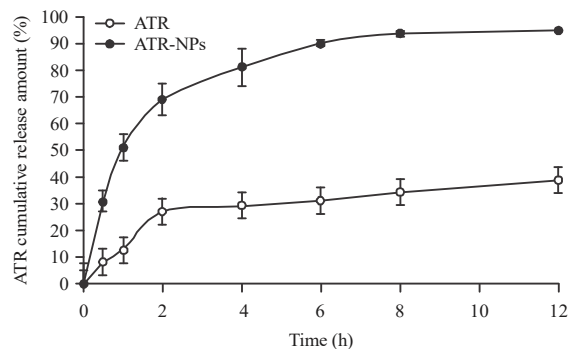


Fig. 2: ATR cumulative release (%) of raw ATR and ATR-NPs

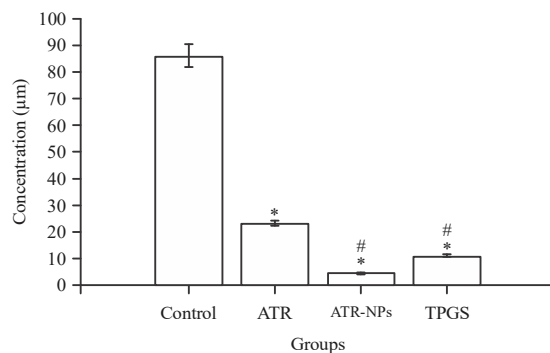


Fig. 3:  $IC_{50}$  of the control, raw ATR and the ATR NPs in the HepG2 cell line

\*Significantly different ( $p < 0.05$ ) compared to control, #Significantly different ( $p < 0.05$ ) compared to raw ATR

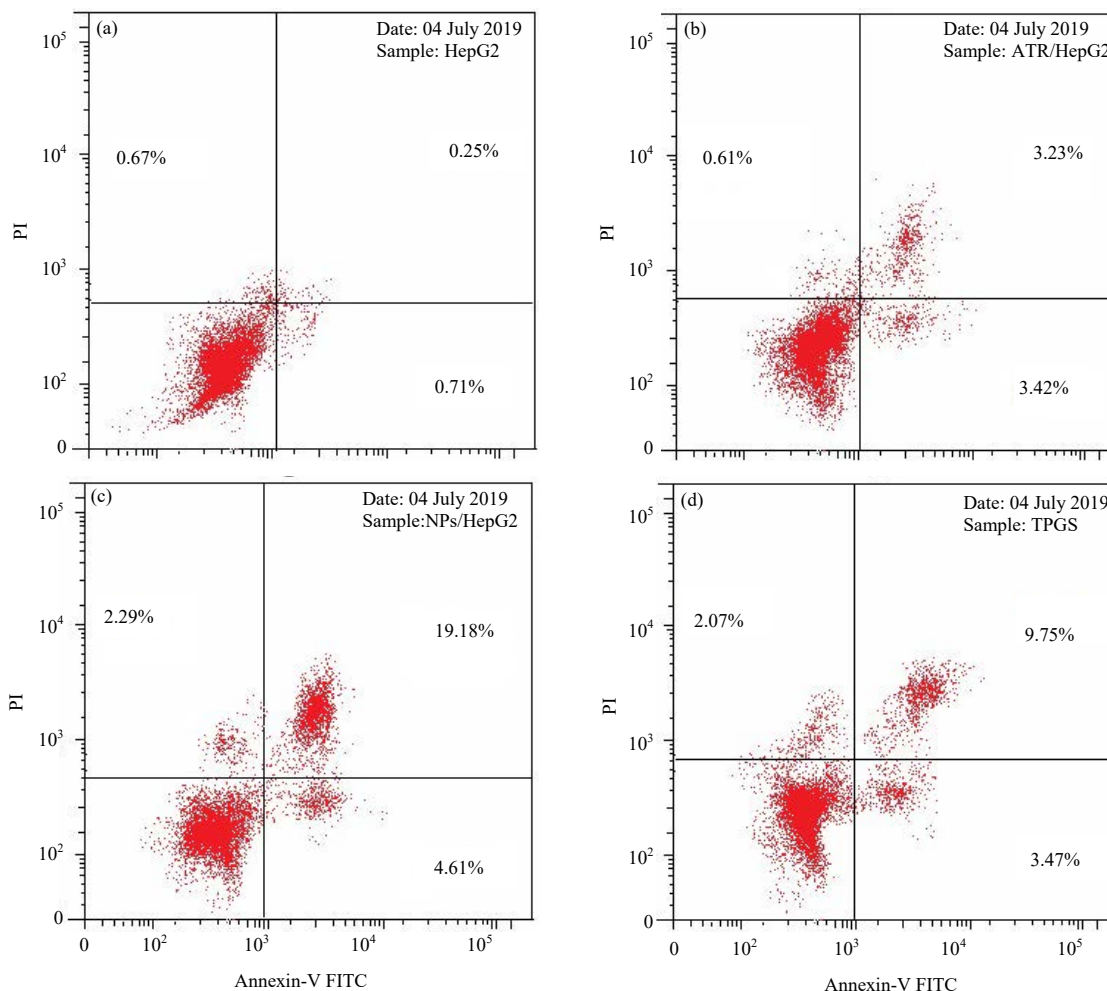


Fig. 4(a-d): Effect of the a HepG2 cells without treatments, (a) raw ATR, (b) ATR NPs, (c) TPGS and (d) Control treatments on the percentage of annexin V-FITC positive staining in HepG2 cells

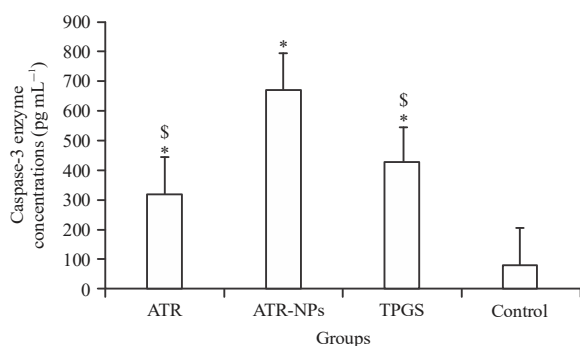


Fig. 5: Caspase-3 enzyme concentrations in HepG2 cells, raw ATR, ATR NPs and TPGS control treatments

Value indicate the Mean±SD (n = 3), \*p<0.05 ATR, ATR NPs and TPGS compared to control, \*\*p<0.05 ATR, TPGS compared to ATR-NPs

## DISCUSSION

The results of this study revealed that the particles were distinct, closely packed, spherical and of a uniform size. The high encapsulation efficiency of ATR-NPs and their physical characteristics offer therapeutic benefits. These benefits were enhanced by the ATR-NPs releasing their contents in a sustained manner, making them useful interventions to target tumors. The chemotherapeutic effect of the drugs was promoted by the internalization of the nanoparticles in a time-dependent manner, as the drugs can accumulate to effective quantities in the intracellular environment. The cytotoxic potential of ATR-NPs was higher than free ATR, as demonstrated by the *in vitro* cytotoxicity experiments conducted using different cancer cell line. The IC<sub>50</sub> values for HepG2 cell lines were lower than other cell lines. These results

indicated the efficacy of nanoparticle formulations for the treatment of cancer. In response to the Bax-mediated mitochondrial pathway, ATR initiated the secretion of cytochrome c into the cytosol, instigating cell death<sup>18,38-42</sup>. Different cell lines showed different levels of cytotoxicity. The zeta potential value indicated the degree of the dispersed phase's electrostatic repulsion and thus the stability in the dispersion medium<sup>32</sup>. The ATR is hydrophobic and therefore, provides good properties for ATR in NPs, which is possibly the cause of the high efficiency of encapsulation observed. A biphasic sustained permeation pattern was indicated by the examination of the permeation properties of the prepared ATR-NPs formula. The rapid release of the product stuck to the surface of the NPs is often the trigger of the initial burst impact phase, with release becoming much slower as the drug has to follow the longer path of diffusion of the more engrained ATR in the central matrix of the polymer. The data in the published literature indicates that ATR and ATR derivatives can exert potent cytotoxic activity upon diverse human cancer cell lines<sup>33,34</sup>. This points to an off-label potential for ATR to be used as a chemopreventive agent in for cancer<sup>35,36</sup>. However, the high hydrophobicity of ATR presents a significant hurdle to using ATR as a chemotherapy agent<sup>37,38</sup>. Despite the potential, little attempt has been made to resolve this limitation. This pioneering study presents a novel drug delivery system, in which PLGA-based nanoparticles are emulsified with TPGS to facility the delivery of an ATR cargo. Cytochrome c is an essential protein in the electron transport chain, situated on the inner membrane of mitochondria, where it performs oxidation and reduction reactions. In apoptosis, cytochrome c binds to cardiolipin on the outer membrane of mitochondria<sup>28,39</sup>. Due to the significant positive charge on cytochrome C its initial interaction with cardiolipin is electrostatic, but its final interaction is hydrophobic. Cardiolipin has a hydrophobic tail that inserts itself into cytochrome c's hydrophobic portion. Also, a cardiolipin-specific oxygenase oxidizes cardiolipin to form cardiolipin hydroperoxides, which are transferred from the inner to the outer membrane<sup>40-43</sup>. This transportation creates pores in the mitochondrial membrane, which enable cytochrome c to escape into the cytosol. Here, cytochrome C binds to an IP3 receptor on the endoplasmic reticulum, activating the intracellular release of calcium<sup>44,45</sup>. Cell death ensues when the levels of calcium levels become toxic. The release of cytochrome c also activates caspase 9, which in turn activates caspase 3 and caspase 7 that destroy the cell from within. Cofilin is activated by small G proteins that are down regulated in the presence of statins. Cofilin is involved in stabilizing the cell's morphology and motility, which in turn

minimizes cholesterol and the components of lipid rafts<sup>44,46,47</sup>. When cofilin is inactivated, the cell becomes unable to form the caveolae (membranous pits) that precede cellular transport and contributed to cellular shape and motility. Based upon existing data, we infer that loss of cholesterol associated isoprenylation promotes morphological changes from which the cell cannot recover, therefore, it dies<sup>48,49</sup>.

## CONCLUSION

The 1:1 ratio of ATR: PLGA with TPGS emulsifier was used in this study to synthesize ATR-NPs. The products exhibited potent cellular cytotoxicity, being 6 times greater than raw ATR. A caspase 3 enzyme assay verified the results, demonstrating a two-fold increase compared to raw ATR. Similarly, cell cycle analysis revealed the pre-G1 phase increase by approximately 1.3-times more than raw ATR. Thus, cell apoptosis was induced more readily and cytotoxicity was increased. These findings suggest this formula is a promising therapy for patients with liver cancer.

## SIGNIFICANCE STATEMENT

This study discovered the Novel combination of ATR with TPGS that can be beneficial for management of liver cancer. This study will help the researcher to uncover the critical areas of using statins as a protective agents against many cancer types, which a new recommendation, in addition to understanding the unique characters of the statins specially mechanisms and selectivity of these drugs. Thus a new recommendation on using of statins may be advised.

## ACKNOWLEDGMENT

The authors extend their appreciation to the Deanship of Scientific Research, at King Khalid University for funding this work through General Research, Project under grant number (GRP-284-40).

## REFERENCES

1. Torre, L.A., F. Bray, R.L. Siegel, J. Ferlay, J. Lortet-Tieulent and A. Jemal, 2015. Global cancer statistics, 2012. CA: Cancer J. Clin., 65: 87-108.
2. Johnell, O. and J.A. Kanis, 2006. An estimate of the worldwide prevalence and disability associated with osteoporotic fractures. *Osteoporosis Int.*, 17: 1726-1733.
3. Tran, S., P.J. DeGiovanni, B. Piel and P. Rai, 2017. Cancer nanomedicine: A review of recent success in drug delivery. *Clin. Transl. Med.*, Vol. 6, No. 1. 10.1186/s40169-017-0175-0.

4. Kerbel, R.S., 1991. Inhibition of tumor angiogenesis as a strategy to circumvent acquired resistance to anti-cancer therapeutic agents. *BioEssays*, 13: 31-36.
5. Donelli, M.G., M. Zucchetti and M. D'Incalci, 1992. Do anticancer agents reach the tumor target in the human brain? *Cancer Chemother. Pharmacol.*, 30: 251-260.
6. Kwon, I.K., S.C. Lee, B. Han and K. Park, 2012. Analysis on the current status of targeted drug delivery to tumors. *J. Controlled Release*, 164: 108-114.
7. Barratt, G.M., 2000. Therapeutic applications of colloidal drug carriers. *Pharmaceut. Sci. Technol. Today*, 3: 163-171.
8. Jokerst, J.V., T. Lobovkina, R.N. Zare and S.S. Gambhir, 2011. Nanoparticle PEGylation for imaging and therapy. *Nanomedicine*, 6: 715-728.
9. Tisato, F., C. Marzano, M. Porchia, M. Pellei and C. Santini, 2010. Copper in diseases and treatments and copper-based anticancer strategies. *Med. Res. Rev.*, 30: 708-749.
10. Brown, A.J., 2007. Cholesterol, statins and cancer. *Clin. Exp. Pharmacol. Physiol.*, 34: 135-141.
11. Mailman, T., M. Hariharan and B. Karten, 2011. Inhibition of neuronal cholesterol biosynthesis with lovastatin leads to impaired synaptic vesicle release even in the presence of lipoproteins or geranylgeraniol. *J. Neurochem.*, 119: 1002-1015.
12. Nolting, S., J. Maurer, G. Spottl, E.T.A. Prada and C. Reuther *et al.*, 2015. Additive anti-tumor effects of lovastatin and everolimus *in vitro* through simultaneous inhibition of signaling pathways. *PLoS ONE*, Vol. 10. 10.1371/journal.pone.0143830.
13. Matuszewicz, L., J. Meissner, M. Toporkiewicz and A.F. Sikorski, 2015. The effect of statins on cancer cells. *Tumor Biol.*, 36: 4889-4904.
14. Waldman, A. and L. Kritharides, 2003. The pleiotropic effects of HMG-Coa reductase inhibitors: Their role in osteoporosis and dementia. *Drugs*, 63: 139-152.
15. Karlic, H., R. Thaler, C. Gerner, T. Grunt, K. Proestling, F. Haider and F. Varga, 2015. Inhibition of the mevalonate pathway affects epigenetic regulation in cancer cells. *Cancer Genet.*, 208: 241-252.
16. Reiss, A.B. and E. Wirkowski, 2007. Role of HMG-CoA reductase inhibitors in neurological disorders. *Drugs*, 67: 2111-2120.
17. Buranrat, B., L. Senggunprai, A. Prawan and V. Kukongviriyapan, 2016. Simvastatin and atorvastatin as inhibitors of proliferation and inducers of apoptosis in human cholangiocarcinoma cells. *Life Sci.*, 153: 41-49.
18. Fahmy, U.A. and B.M. Aljaeid, 2016. Combined strategy for suppressing breast carcinoma MCF-7 cell lines by loading simvastatin on alpha lipoic acid nanoparticles. *Expert Opin. Drug Deliv.*, 13: 1653-1660.
19. Suroliya, R., M. Pachauri and P.C. Ghosh, 2012. Preparation and characterization of monensin loaded PLGA nanoparticles: *In vitro* anti-malarial activity against *Plasmodium falciparum*. *J. Biomed. Nanotechnol.*, 8: 172-181.
20. Dong, Y. and S.S. Feng, 2005. Poly(D,L-lactide-co-glycolide)/montmorillonite nanoparticles for oral delivery of anticancer drugs. *Biomaterials*, 26: 6068-6076.
21. Ghahremankhani, A.A., F. Dorkoosh and R. Dinarvand, 2007. PLGA-PEG-PLGA tri-block copolymers as an *in-situ* gel forming system for calcitonin delivery. *Polym. Bull.*, 59: 637-646.
22. Yoo, H.S. and T.G. Park, 2001. Biodegradable polymeric micelles composed of doxorubicin conjugated PLGA-PEG block copolymer. *J. Controlled Release*, 70: 63-70.
23. Yang, C., T. Wu, Y. Qi and Z. Zhang, 2018. Recent advances in the application of vitamin E TPGS for drug delivery. *Theranostics*, 8: 464-485.
24. Guo, Y., J. Luo, S. Tan, B.O. Otieno and Z. Zhang, 2013. The applications of vitamin E TPGS in drug delivery. *Eur. J. Pharm. Sci.*, 49: 175-186.
25. Varma, M.V.S. and R. Panchagnula, 2005. Enhanced oral paclitaxel absorption with vitamin E-TPGS: Effect on solubility and permeability *in vitro*, *in situ* and *in vivo*. *Eur. J. Pharmaceut. Sci.*, 25: 445-453.
26. Ahmed, O.A., U.A. Fahmy, A.S. Al-Ghamdi, B.M. Aljaeid and H. Aldawsari *et al.*, 2017. Finasteride-loaded biodegradable nanoparticles: Near-infrared quantification of plasma and prostate levels. *J. Bioact. Compatible Polym.*, 32: 557-567.
27. Radwan, M.F., M.A. El-Moselhy, U.A. Fahmy and B.M. Aljaeid, 2019. Novel combination of alprostadil-D-tocopheryl polyethylene glycol succinate for treatment of erectile dysfunction. *Int. J. Pharmacol.*, 15: 738-744.
28. Mylonaki, I., O. Trosi, E. Allemann, M. Durand, O. Jordan and F. Delie, 2018. Design and characterization of a perivascular PLGA coated PET mesh sustaining the release of atorvastatin for the prevention of intimal hyperplasia. *Int. J. Pharmaceut.*, 537: 40-47.
29. Fahmy, U.A. and H. Aldawsari, 2018. Combined ceftriaxone sodium with alpha lipoic acid nanoliposomes for more stable and less nephrotoxic formula in pediatrics. *Digest J. Nanomater. Biostruct.*, 13: 245-252.
30. Kurakula, M., O.A.A. Ahmed, U.A. Fahmy and T.A. Ahmed, 2016. Solid lipid nanoparticles for transdermal delivery of avanafil: Optimization, formulation, *in-vitro* and *ex-vivo* studies. *J. Liposome Res.*, 26: 288-296.
31. Fahmy, U.A., 2018. Augmentation of fluvastatin cytotoxicity against prostate carcinoma PC3 cell line utilizing alpha lipoic-ellagic acid nanostructured lipid carrier formula. *AAPS PharmSciTech*, 19: 3454-3461.

32. Ahmed, T.A., K.M. El-Say, B.M. Aljaeid, U.A. Fahmy and F.I. Abd-Allah, 2016. Transdermal glimepiride delivery system based on optimized ethosomal nano-vesicles: Preparation, characterization, *in vitro*, *ex vivo* and clinical evaluation. *Int. J. Pharmaceut.*, 500: 245-254.
33. Prabhakar, P.V., U.A. Reddy, S.P. Singh, A. Balasubramanyam and M.F. Rahman *et al.*, 2012. Oxidative stress induced by aluminum oxide nanomaterials after acute oral treatment in Wistar rats. *J. Applied Toxicol.*, 32: 436-445.
34. Gambhire, V.M., S.M. Salunkhe and M.S. Gambhire, 2018. Atorvastatin-loaded lipid nanoparticles: Antitumor activity studies on MCF-7 breast cancer cells. *Drug Dev. Ind. Pharm.*, 44: 1685-1692.
35. Alizadeh-Tabrizi, N., H. Malekinejad, S. Varasteh and H. Cheraghi, 2017. Atorvastatin protected from paraquat-induced cytotoxicity in alveolar macrophages *via* down-regulation of TLR-4. *Environ. Toxicol. Pharmacol.*, 49: 8-13.
36. Shu, N., M. Hu, Z. Ling, P. Liu and F. Wang *et al.*, 2016. The enhanced atorvastatin hepatotoxicity in diabetic rats was partly attributed to the upregulated hepatic Cyp3a and SLCO1B1. *Scient. Rep.*, Vol. 6. 10.1038/srep33072.
37. Huichun, J.I., J. Liu, Y. Zhou, Y. Li, F. Chen and S. Fei, 2017. Effect and mechanism of atorvastatin on cytotoxicity of human NK cells to colon cancer cells. *Chin. J. Immunol.*, 33: 178-185.
38. Fahmy, U.A., 2016. Quantification of simvastatin in mice plasma by near-infrared and chemometric analysis of spectral data. *Drug Des. Dev. Ther.*, 10: 2507-2513.
39. Oliveira, K.A., T. Dal-Cim, F.G. Lopes, F.K. Ludka, C.B. Nedel and C.I. Tasca, 2018. Atorvastatin promotes cytotoxicity and reduces migration and proliferation of human A172 glioma cells. *Mol. Neurobiol.*, 55: 1509-1523.
40. Hwang, K.E., K.S. Na, D.S. Park and K.H. Choi *et al.*, 2011. Apoptotic induction by simvastatin in human lung cancer A549 cells via Akt signaling dependent down-regulation of survivin. *Invest. New Drugs*, 29: 945-952.
41. Hardie, C., Y. Jung and M. Jameson, 2016. Effect of statin and aspirin use on toxicity and pathological complete response rate of neo-adjuvant chemoradiation for rectal cancer. *Asia-Pac. J. Clin. Oncol.*, 12: 167-173.
42. Dorsam, B., A. Goder, N. Seiwert, B. Kaina and J. Fahrner, 2015. Lipoic acid induces p53-independent cell death in colorectal cancer cells and potentiates the cytotoxicity of 5-fluorouracil. *Arch. Toxicol.*, 89: 1829-1846.
43. Ukomadu, C. and A. Dutta, 2003. p21-dependent inhibition of colon cancer cell growth by mevastatin is independent of inhibition of G<sub>1</sub> cyclin-dependent kinases. *J. Biol. Chem.*, 278: 43586-43594.
44. Orrenius, S., 2019. Role of cell death in toxicology: Does it matter how cells die? *Annu. Rev. Pharmacol. Toxicol.*, 59: 1-14.
45. Hedger, G., H. Koldso, M. Chavent, C. Siebold, R. Rohatgi and M.S.P. Sansom, 2019. Cholesterol interaction sites on the transmembrane domain of the hedgehog signal transducer and class FG protein-coupled receptor smoothed. *Structure*, 27: 549-559.
46. Szeto, H.H., 2017. Pharmacologic approaches to improve mitochondrial function in AKI and CKD. *J. Am. Soc. Nephrol.*, 28: 2856-2865.
47. Yeganeh, B., E. Wiechec, S.R. Ande, P. Sharma and A.R. Moghadam *et al.*, 2014. Targeting the mevalonate cascade as a new therapeutic approach in heart disease, cancer and pulmonary disease. *Pharmacol. Therapeut.*, 143: 87-110.
48. Rouviere, E., C. Arnarez, L. Yang and E. Lyman, 2017. Identification of two new cholesterol interaction sites on the A<sub>2A</sub> adenosine receptor. *Biophys. J.*, 113: 2415-2424.
49. Shamas-Din, A., S. Bindner, X. Chi, B. Leber, D.W. Andrews and C. Fradin, 2015. Distinct lipid effects on tBid and Bim activation of membrane permeabilization by pro-apoptotic Bax. *Biochem. J.*, 467: 495-505.